

# Coupled Electric Drives Data Set and Reference Models

Technical Reports from the department of Information Technology 2017-024, Uppsala University,  
Uppsala, Sweden, December, 2017

Torbjörn Wigren<sup>1</sup> and Maarten Schoukens<sup>2</sup>

<sup>1</sup> Division of Systems and Control, Department of Information Technology, Uppsala University, SE  
75105 Uppsala, Sweden. e-mail: [torbjorn.wigren@it.uu.se](mailto:torbjorn.wigren@it.uu.se).

<sup>2</sup> Control Systems Group, Eindhoven University of Technology, Eindhoven, The Netherlands. e-mail:  
[m.schoukens@tue.nl](mailto:m.schoukens@tue.nl).

## Abstract

The following report provides a description of the CE8 coupled electric drives laboratory process. A first set of continuous time model structures that are suitable to describe the nonlinear dynamics are presented. The data sets, which are available in .mat and .csv file formats, are then described in detail. The available data sets are short, which constitute a challenge when performing identification. In support of future work, Wiener models are identified with a recursive algorithm that is parameterized in continuous time. This approach reduces the number of parameters to four for identification of third order dynamics.

## 1. The Coupled Electric Drives

### 1.1 Overview

The CE8 coupled electric drives [1] consists of two electric motors that drive a pulley using a flexible belt. The system is depicted in Fig. 1. The pulley is held by a spring, resulting in a lightly damped dynamic mode. The electric drives can be individually controlled allowing the tension and the speed of the belt to be simultaneously controlled. The drive control is symmetric around zero, hence both clockwise and counter clockwise movement is possible. Here the focus is only on the speed control system. The reason is that the angular speed of the pulley is measured with a pulse counter and this sensor is *insensitive to the sign of the velocity*. Following the sensor, analogue low pass filtering and anti-aliasing filtering is applied. The dynamic effects are generated by the electric drive time constants, the spring and the analogue low pass filtering. The latter has a quite limited effect on the output and may be neglected.

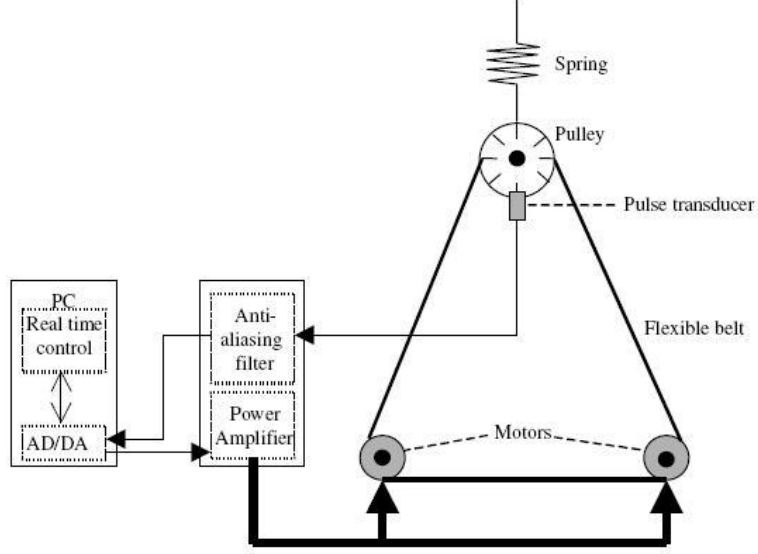


Fig. 1: The CE8 coupled electric drives.

## 1.2 Wiener model

By considering the sum of the voltages applied to the motors as the input signal  $u(t)$ , physical modeling results in a lightly damped linear third order system, as measured from voltages to the pulley velocity  $y(t)$ . A first continuous time description of the linear dynamic part of the system is therefore given by

$$y(s) = \frac{k\alpha\omega_0^2}{(s + \alpha)(s^2 + 2\xi\omega_0s + \omega_0^2)} u(s). \quad (1)$$

Here  $\alpha$  denotes the inverse time constant of the electric drives,  $\xi$  denotes the damping related to the spring and the flexible belt,  $\omega_0$  denotes the angular resonance frequency, and  $k$  denotes the static gain.

The pulley velocity is rectified by the pulse counter to give the speed, after which it is filtered with an anti-aliasing filter. For the first model the filtering is neglected. The measured output speed after rectification therefore becomes

$$y_n(t) = |y(t)| + e(t), \quad (2)$$

where  $y_n(t)$  denotes the measured output speed signal and where  $e(t)$  denotes a measurement disturbance. The signal  $y(t)$  is not available for measurement. Equations (1) – (2) clearly represents a Wiener model [2]. Generalizations include e.g. addition of a disturbance to  $y(t)$  before rectification.

### 1.3. Wiener – Hammerstein model

The exact model of the analogue anti-aliasing filtering is not known, however the bandwidth is close to 12 Hz. This is less than the sensor bandwidth. In order to include modeling of the anti-aliasing filter, a continuous time Wiener – Hammerstein model [2] is suitable. For the coupled electric drives this models may be written as

$$y(s) = \frac{k\alpha\omega_0^2}{(s + \alpha)(s^2 + 2\xi\omega_0s + \omega_0^2)} u(s) \quad (3)$$

$$z(t) = |y(t)| \quad (4)$$

$$y_n(s) = \frac{b_1s^{n-1} + \dots + b_n}{s^n + a_1s^{n-1} + \dots + a_n} z(s) + v(s). \quad (5)$$

Here  $y(t)$  and  $z(t)$  are not available for measurement, and  $v(t)$  denotes a measurement disturbance. Note that there is a static gain ambiguity in the formulation of (3)-(5) unless the unknown anti-aliasing dynamics is restricted to give a static gain of (1). Generalizations include addition of disturbances to  $y(t)$  and  $z(t)$ . The identification of the system based on the Wiener – Hammerstein models using the present data set is a topic for further research.

### 1.4. Other models

As will become clear below, at least the Wiener model leaves some un-modeled dynamics after identification. Such dynamics may be captured by identification of more advanced models, e.g. nonlinear state space models [3], [4]. Also this is a topic for further research.

## 2. The Measured Data Sets

### 2.1 PRBS input signal

The first type of input signal was a PRBS with a clock period of 5 times the sampling period. The signal was switching between  $-u_{PRBS}$  V and  $+u_{PRBS}$  V, resulting in the process changing the belt rotation direction frequently. Three open loop realizations were recorded for  $u_{PRBS} = 0.5, 1.0, 1.5$ . The input-output data was collected with a sampling period of 20 ms. Note that the 50 Hz sampling frequency is significantly higher than the bandwidth of the anti-aliasing filter. The durations of the measurement were 10 s, resulting in 500 input-output samples for each set of data. The input-output data obtained from the first realization of the uniformly distributed input signal is depicted in Fig. 2.

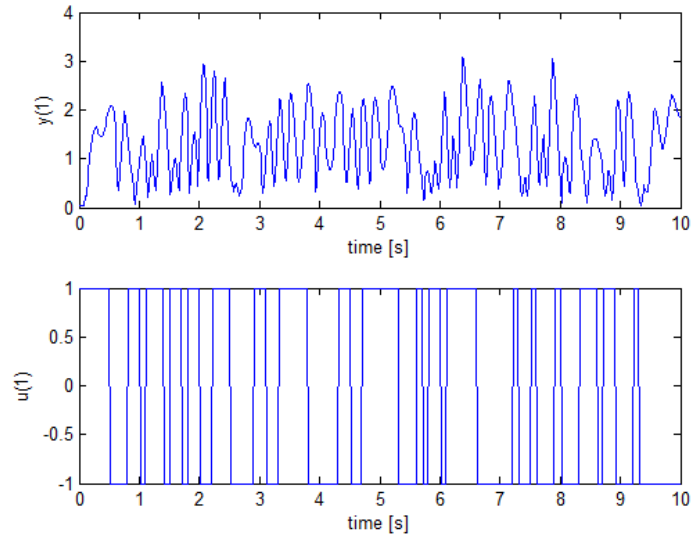


Fig. 2: Input-output data from the coupled electric drives speed system.

## 2.2 Uniformly distributed input signal

The second type of input signal was obtained from a PRBS with a clock period of 5 times the sampling period, switching between  $-1.5$  V. and  $+2.5$  V, as well as between  $-1.0$  V and  $+3.0$  V. The signal in each clock interval of constant signal level, was then multiplied with a random number, uniformly distributed in amplitude between 0 and 1. The resulting input signal is then uniformly distributed in amplitude. The reason for this input signal is that when the system is nonlinear, both the frequency and amplitude contents of the input signal are important for identification [5]. The input-output data was again recorded with a sampling period of 20 ms. The durations of the measurement were 10 s, resulting in 500 input-output samples for each set of data. The input-output data obtained from the first realization of the uniformly distributed input signal is depicted in Fig. 3.

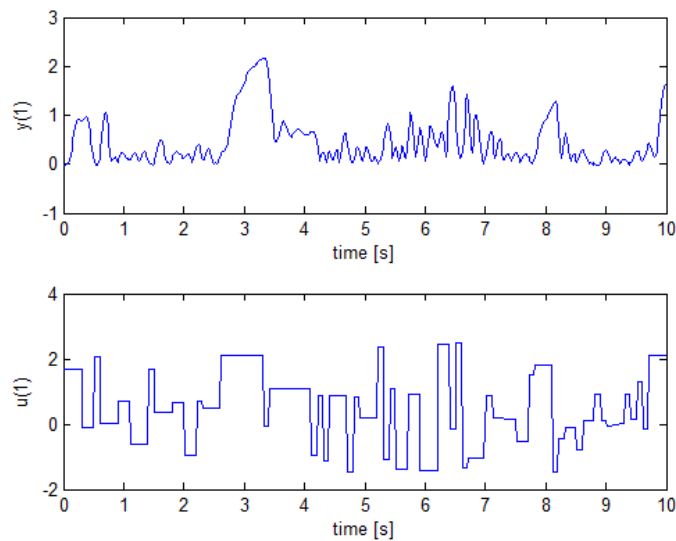


Fig. 3: Input-output data from the coupled electric drives speed system.

## 2.3 Loading

The data sets are available in the form of .MAT files, directly loadable into MATLAB™. There are three PRBS data sets distinguished with the input data numbers as u1, u2 and u3. The corresponding outputs are z1, z2, and z3, not to be confused with (4). There are two uniform data sets distinguished with the input data numbers u11 and u12. The corresponding outputs are z11 and z12. All quantities are row vectors.

The PRBS data is stored in the file DATAPRBS.MAT and the uniform data is stored in the file DATAUNIF.MAT. They are loaded into MATLAB™ with the load command. The data is also available in .CSV format.

## 3. Identified Reference Models

### 3.1 Identification algorithm and parameterization

This section presents results for the recursive Wiener identification case, assuming that the output nonlinearity is known to be given by (2). The data sets may of course be used without inferring this a priori knowledge, for example for benchmarking purposes.

The RPEM algorithm of [3] was used for recursive identification of the system. That algorithm is based on a continuous time nonlinear state space ODE model, where one right hand side component is modeled by a multi-dimensional polynomial in the states and input variables. The parameters are the coefficients of the polynomial, see [3] for details.

The output signal of the RPEM of [3] is generated as a known nonlinear transformation of the state and input signals. By restriction of the polynomial right hand to include only terms that are linear in the states and inputs, the RPEM of [3] can be used for recursive identification using the model structure of (1) and (2). The following model structure selection results, where the notation of [3] is applied,

$$\begin{pmatrix} \dot{x}_1 \\ \dot{x}_2 \\ \dot{x}_3 \end{pmatrix} = \begin{pmatrix} x_2 \\ x_3 \\ \theta_{0001}u + \theta_{0010}x_3 + \theta_{0100}x_2 + \theta_{1000}x_1 \end{pmatrix} \quad (6)$$

$$y(t) = |x_1(t)|. \quad (7)$$

Straightforward computations show that

$$x_1(s) = \frac{\theta_{0001}}{s^3 - \theta_{0010}s^2 - \theta_{0100}s - \theta_{1000}} u(s). \quad (8)$$

Note that the number of unknown parameters is 4 with the continuous time parameterization while it would be 6 for a discrete time model. In addition, the parameters can be used to solve for the physical quantities of (1) using an equation solver for nonlinear equations.

### 3.2 Algorithm tuning

The free SW package [6] that implements the RPEM of [3] together with a variety of supporting functions was used to generate the results below. The details of the setting of the algorithm appear in Table 1.

Parameter	Value	Appears in file	Meaning
nu	1	SetupLive.m	# Inputs
nx	3	SetupLive.m	# States
ny	1	SetupLive.m	# Outputs
Ts	0.020	SetupLive.m	Sampling period
N	500	SetupLive.m	Data length
x_m_0	$(-1.0 \ 0.0 \ 0.0)^T$	SetupRPEM	Initial state
mu_Factor	200	SetupRPEM	Part of gain sequence
mu_0	5	SetupRPEM	Part of gain sequence
mu0	0.9999	SetupRPEM	Part of gain sequence
initialNoiseVariance	0.01	SetupRPEM	Initial value of RPEM
scaleFactorR	$0.5 / \hat{\theta}_{1000}(0)$	SetupRPEM	Initial size of Hessian
stabilityLimit	0.995	SetupRPEM	Projection limit
scalingTS	10	SetupRPEM	Sampling scale factor [4]

Table 1: The parameters set for the identification algorithm. The reader is referred to [3], [4] and [6] for further details of the parameters.

It can be noted that the system has a bandwidth of a few Hz. In order for the algorithm to better condition a scaling of the sampling period of 10 was applied, see [4]. This means that also initial values and the identified parameters become scaled [4]. The advantage is that the scaled parameters are transformed towards 1 where numerical properties are expected to be best. Fortunately, as proved in [4] it is straightforward to recover the un-scaled parameters. Also note that scaleFactorR is scaled with the inverse of the pole radius raised to the model order since that reflects the initial uncertainty when initializing the (scaled) parameters.

### 3.3 Uniform data results

The following results were obtained for the second set of uniform data, using the setting of Table 1. As can be seen the initiation with scaled triple poles in the range -0.75 to -2.5, with a static gain of 1, appear to result in reasonable parameters.

$\hat{\theta}_{scated}(0)$ poles	$\hat{\theta}_{0001}(500)$	$\hat{\theta}_{0010}(500)$	$\hat{\theta}_{0100}(500)$	$\hat{\theta}_{1000}(500)$	$v(500)$
-0.5	-858.8	-21.86	-255.0	-1079	-0.1962
-0.75	1531	-25.08	-406.2	-1826	-0.3385
-1.0	2132	-24.83	-548.0	-2609	-0.4025
-1.5	2567	-23.93	-627.4	-3293	-0.3841
-2.0	2922	-27.09	-668.9	-3834	-0.4010
-2.5	4186	-41.64	-870.8	-5684	-0.3424
-3.0	10370	-124.9	-2694	-23220	0.9163

Table 2: Results for the case the RPEM is initialized with a triple pole in the location of the table.  $V$  denotes the RPEM loss function, c.f. [6].

To illustrate the best result, a Bode diagram is depicted in Fig. 4. The drive dynamics appears to have a bandwidth of a few radians per second while the small resonance peak appears at about 25 radians per second, i.e. at 4-5 Hz. The simulated output of the system is plotted in Fig. 5. The algorithm hence appears to converge quite well in 500 samples when initialized with triple poles in the range from 0.75 to 2.5 radians/s.

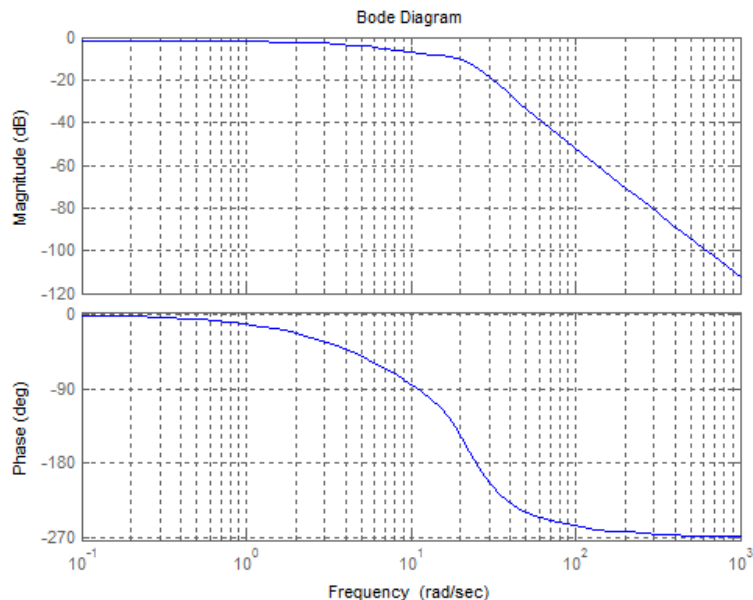


Fig. 4: Bode diagram of the identified model when initiated with a triple pole in -1.

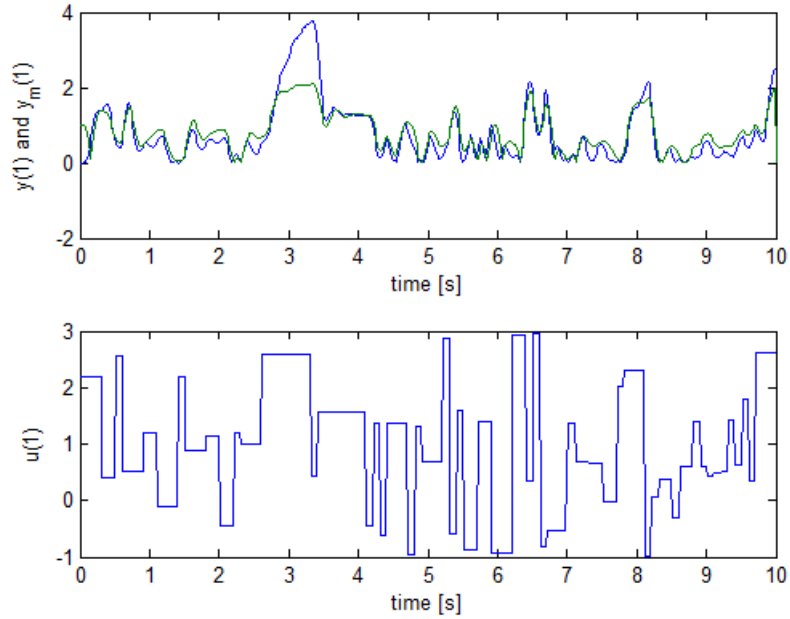


Fig. 5: The simulated model output together with the data, using the parameters obtained at the end of the run.

### 3.4 PRBS data results

The following single result was obtained for the first set of PRBS data, using the setting of Table 1, with the exception that scalingTS was set to 15 and mu0 was set to 0.998. The following result was obtained.

$\hat{\theta}_{scaled}(0)$ poles	$\hat{\theta}_{0001}(500)$	$\hat{\theta}_{0010}(500)$	$\hat{\theta}_{0100}(500)$	$\hat{\theta}_{1000}(500)$	$v(500)$
-0.5	4015	-17.96	-463.7	-2094	-0.2803
-0.75	5163	-19.93	-509.8	-2835	-1.0708
-1.0	5017	-19.61	-504.2	-2747	-1.0027
-1.5	5174	-20.52	-512.5	-2931	-0.6688
-2.0	25991	-87.30	-1703	-16230	-0.0205

4

Table 2: Results for the case the RPEM is initialized with a triple pole in -1. V denotes the RPEM loss function, c.f. [6].

To illustrate the result, a Bode diagram is depicted in Fig. 6. The combined drive dynamics and the small resonance peak appear at about 25 radians per second, i.e. at 4-5 Hz. Note that the static gain is different than in Fig. 4 and that the fit is better, as manifested by the loss function and Fig. 7.



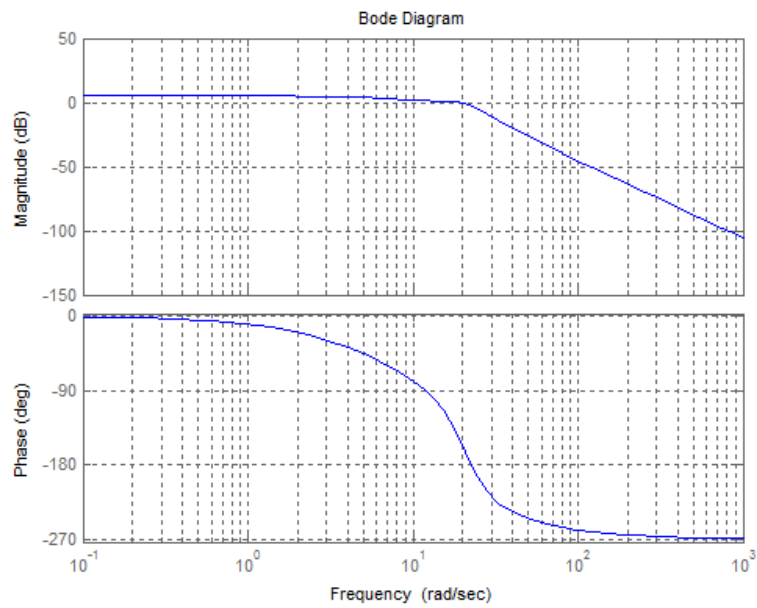


Fig. 6: Bode diagram of the identified model when initiated with a triple pole in -0.75.

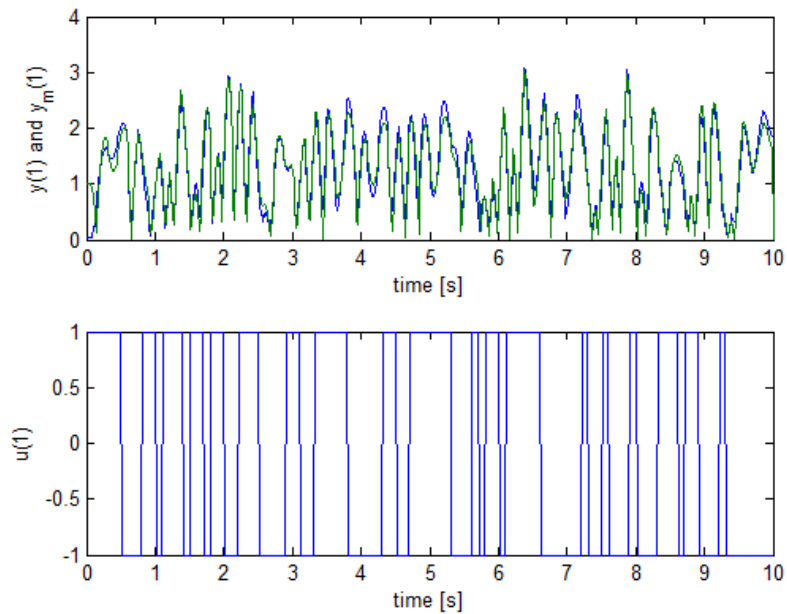


Fig. 7: The simulated model output together with the data, using the parameters obtained at the end of the run.

### 3.5 Effects of sampling

The algorithm of [3], [6] identifies the parameters of a continuous time model, discretized with an Euler method. This means that the continuous time parameters are not fully representative of the identified result, the effect of the sampling needs to be accounted for as

well. Therefore, the continuous time Bode diagrams above are not fully representative of the frequency response of the system either. Note that the reason why the algorithm is constructed in this way is that it is intended to handle a general nonlinear system and not only a Wiener system.

However, in the present case the sampling does have a significant effect on the result. To see this, the discrete time model was retrieved from the RPEM code, by using the matrix  $SM$  to obtain the discrete time eigenvalues. This resulted in the discrete time linear model

$$H(z) = \frac{0.0414}{z^3 - 2.6011z^2 + 2.4060z - 0.7823}. \quad (9)$$

The discrete time Bode plot is depicted in Fig. 8. The small resonance peak is now more clearly visible. The RPEM hence adapts the parameters so that the discretization itself assists in the modeling of the resonant parts of the signal.

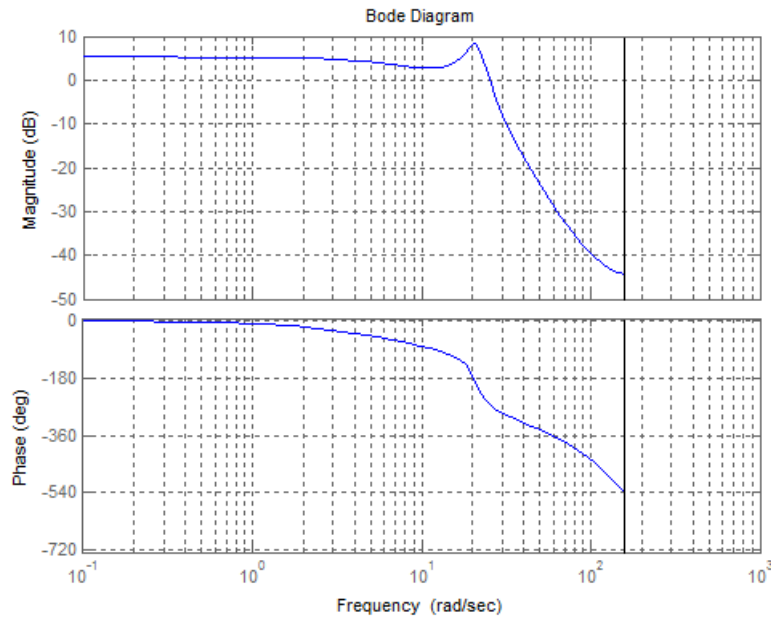


Fig. 8: The Bode plot corresponding to Fig. 6 of the discretized identified linear part of the model of the system.

In the nonlinear case there is no exact correspondence between discrete time and continuous time models by means of mechanisms like ZoH sampling. It is then a good idea to use a model discretized with the Euler method, when simulating and designing controllers. In case a continuous time model or other discretization methods are used, it is recommended that the result is cross checked with the above sampling effect in mind.

#### 4. Concluding remarks

The algorithm is able to produce a quite accurate continuous time Wiener model, despite a short data record and an extreme nonlinearity. As expected, the uniformly distributed input data gave better convergence properties than the PRBS one. However, the simulated output indicates that improvements could be obtained by an application of more advanced modeling techniques.

#### References

- [1] P. E. Wellstead, *Introduction to Physical System Modeling*. Academic Press, London, UK, 1979.
- [2] M. Schoukens and K. Tiels, "Identification of Nonlinear Block-Oriented Systems starting from Linear Approximations: A Survey", *Automatica*, vol. 85, pp. 272-292, 2017.
- [3] T. Wigren, "Recursive identification based on nonlinear state space models applied to drum-boiler dynamics with nonlinear output equations", *Proc. IEEE ACC 2005*, Portland, Oregon, U.S.A., pp. 5066-5072, June 8-10, 2005.
- [4] T. Wigren, "Scaling of the sampling period in nonlinear system identification", *Proc. IEEE ACC 2005*, Portland, Oregon, U.S.A., pp. 5058-5065, June 8-10, 2005.
- [5] T. Wigren, "User choices and model validation in system identification using nonlinear Wiener models", *Prep. 13:th IFAC Symposium on System Identification*, Rotterdam, The Netherlands, pp. 863-868, August 27-29, 2003. Invited session paper.
- [6] T. Wigren, L. Brus and S. Tayamon, "MATLAB software for recursive identification and scaling using a structured nonlinear black-box model - Revision 6", *Technical Reports from the department of Information Technology 2010-022*, Uppsala University, Uppsala, Sweden, September, 2010.